International Journal of Engineering Sciences &Research Technology

(A Peer Reviewed Online Journal)
Impact Factor: 5.164

IJESRT

Chief Editor
Dr. J.B. Helonde

Executive Editor
Mr. Somil Mayur Shah

RESEARCHERID
THOMSON REUTERS

[Karka, *et al.*, 8(9): September, 2019]
IC™ Value: 3.00

ISSN: 2277-9655
Impact Factor: 5.164
CODEN: IJESS7

IJESRT

INTERNATIONAL JOURNAL OF ENGINEERING SCIENCES & RESEARCH TECHNOLOGY

DIGITAL STUDY OF THE BENDING BEHAVIOUR KNOWN AS «3 POINTS» OF TILES OF DIFFERENT SHAPES (FLEMISH, ROMANESQUE AND FLAT) IN CEMENT CONCRETE

Bozabe Renonet Karka[*1] & Bongor Danhrée[2]

[*1]Department of civil engineering, National Superior School of Public Works (ENSTP), N'Djamena, Chad

[2]Department of Fundamental Sciences, National Superior School of Public Works (ENSTP), N'Djamena,Chad

DOI: 10.5281/zenodo.3480563

ABSTRACT

The inadequacy of the experimental devices for testing the mechanical resistance of the tiles used to cover a roof should not be a reason for not properly understanding the problems associated with their bearing capacity and exploitation. This paper presents the results of a numerical study of the "3 point" bending behaviour of tiles of different geometric shapes (Flemish, Romanesque and Flat) in concrete cement. This work is governed by the finite element method implemented in structural computing software. It highlights the behaviour of the charged tiles when we know their geometric characteristics and some physical and mechanical characteristics of the material. This study found that the geometric shape of a tile significantly influences its load behaviour. For a normative load of 50 kg, the three tile shapes have a good bearing capacity because their bending deformations are all lower than the limit deformation of the bending concrete which is 3.5‰ according to the EC2 rules. However, the Flemish tile (0.2‰) bears more than the Romanesque tile (0.3‰) and the Flat tile (0.6‰). The breaking load of the flat tile is approximately 300 kg. As for the normal operating conditions and service life aspects, the compressive limit stress of the concrete (12 Mpa) and the allowable deflection of the tile (0.74 mm) are widely exceeded for the Plate tile (18.31 MPa and 1.01 mm). The Flemish tile (5.28 MPa and 0.24 mm) seems to offer a little more of the best conditions in service than the Romanesque tile (9.11 MPa and 0.16 mm).

KEYWORDS: Tile, bearing capacity, operation, bending, stress, deformation.

1. INTRODUCTION

In the Sahelian regions of Africa, ceramic roofs are preferred over steel or aluminum roofs. These places have high ambient temperatures of up to 50°C in the shade [1]. For example, to cover a building, cement concrete tiles or baked clay tiles are encouraged because, on the one hand, these tiles are easy to produce and economical because of the use of local materials and on the other hand, they ensure thermal and acoustic comfort. In construction, three types of cement concrete tiles are generally used: The Ordinary Concrete Tile (TBO), manufactured by industrialists; the Fibro - Mortar Tile (TFM) which consists of making a tile produced with a cement mortar, to which small quantities of natural or synthetic fibers are added and the Vibrating Mortar Tile (TMV) where small-diameter aggregates replace fibers. The shapes are very varied, the dimensions also, and are specific to each manufacturer. In the markets, we find Flemish tiles (Figure 1) whose cross-sectional profile is a sinusoid consisting of a concave part and a convex part allowing longitudinal embossing; Romanesque tiles (Figure 2) whose cross-sectional profile consists of a concave part, a flat part and a half - concave part for longitudinal embossing and Flat tiles [2]. When these tiles are stressed by maintenance loads for example, we see a large number of breaks. In general, the manufacturer does not even have adequate technical equipment to test their mechanical resistance (bending, heel traction, impact or impact, sound, etc.). The behaviour of the tiles under load is completely ignored. However, a tile supported by two consecutive structural failures, subjected to a bending load, can be considered a plate or a flexural shell called a “3 point” [3]. The finite element method (MEF) proposed in this study is a simple and practical numerical method for describing and explaining the behaviour of the charged tiles [4-7]. The tile modeling and the simulation of its behaviour are performed by the structural calculation software Autodesk Robot Structural Analysis Professional 2016 [8-11]. Three different

IJESRT is licensed under a Creative Commons Attribution 4.0 International License.

ISSN: 2277-9655
Impact Factor: 5.164
CODEN: IJESS7

forms of TMV tiles with the same support and loading conditions were subjected to linear static analysis [12-13]. An experimental device (Figure 5) was used to validate the results. Information resulting from the interpretation of the results of stress and deformation fields, movement and rotation fields will no doubt help manufacturers to improve their manufacturing techniques and users to make a better choice in tile shapes.

2. MATERIALS AND METHODS

2.1 Mechanical characteristics of concrete

- ***Elasticity***
  - Young module E = 30,000 MPa
  - Poisson coefficient ν = 0.2
  - Shear module G = 12,500 MPa
  - Specific weight $\Upsilon = 25$ kN/m^3
  - Thermal expansion 0.000010 (1/^{0}C)
  - Damping coefficient 0.04
- ***Resistance***
  - Compression Fc28 = 20 MPa
  - Cylindrical sample
- ***Production of tiles***

The production of TMV is carried out according to the methods acquired from the training courses by the LOCOMAT and DECO projects [14]. The tiles produced are of the Flemish, Romanesque and Flat type with the following dimensions:

- Nominal size: 25 cm x 50 cm = 0.125 m²
- Cover area: 0.045 m²/tile
- Useful size: 20 cm x 40 cm = 0.08 m² or 12.5 tiles/m²
- Thickness e 8 mm
- Raw Materials: water (drinkable) + cement (CPA or CPJ) + sand and gravel (siliceous or mineral) + Dyes (red oxide)
- Proportions water/cement: between 0.5 and 0.65 by weight
- Cement dosage: 350 kg/m^3
- Dye content: 3 - 10% of cement weight
- Volume Determination: 2 sands + 1 gravel + 1 cement
- Vibration: 20 - 50 seconds
- Granulometry of mortar aggregates (Table 1).

Tableau 1: Dosage en granulates

Diameter		
Φ_{max}	5,5 mm	
$\Phi > 2$ mm	30 - 50%	gravel
$0,5 < \Phi < 2$ mm	10 - 55%	
$\Phi < 0,5$ mm	15 - 40%	sand

2.2 Tile Operations: Boundary Conditions

- ***Type of tile support***
  - Flemish: Two single supports on the left longitudinal edge and two joints representing the heels on the convex lower part;
  - Romanesque: Two joints representing the heels on the flat lower part and simple supports on the left longitudinal edge and inside the flat part;
  - Flat: Two joints in the middle representing heels and single supports.
- ***Loading type and normative values***
  - Flemish and Romanesque: Punctual 2 x 25 kg = 50 kg;
  - Plate: Linear uniform 50 kg / 0, 25 m = 200 kg/m = 2 kN/m

IJESRT is licensed under a Creative Commons Attribution 4.0 International License.

ISSN: 2277-9655
Impact Factor: 5.164
CODEN: IJESS7

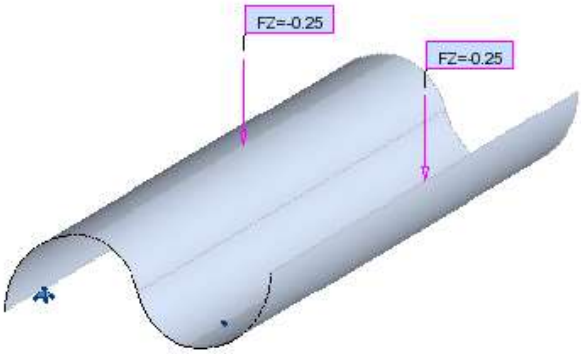

Figure 1: *Flemish Tile*

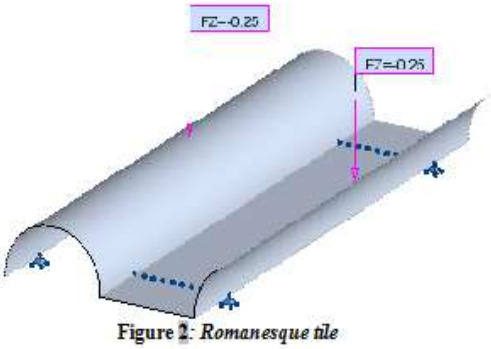

Figure 2: *Romanesque tile*

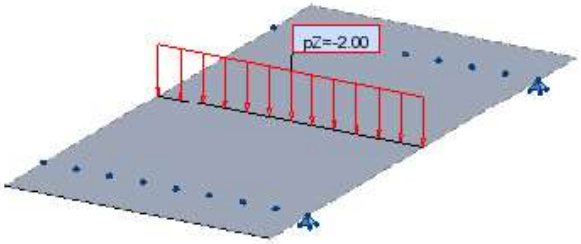

Figure 3: Flat tile

2.3 Brief overview of the "3 point" flexural test

The experimental device adopted is that of the "3 point" bending shown in Figures 4 and 5. This is a conventional mechanical test used to test the bending resistance. This device represents the case of a beam laid on two simple supports and subjected to a concentrated load, applied in the middle of the beam with it also a simple contact. One of the supports is often modeled as a joint in order to have a beam that does not move horizontally (Figure 6).

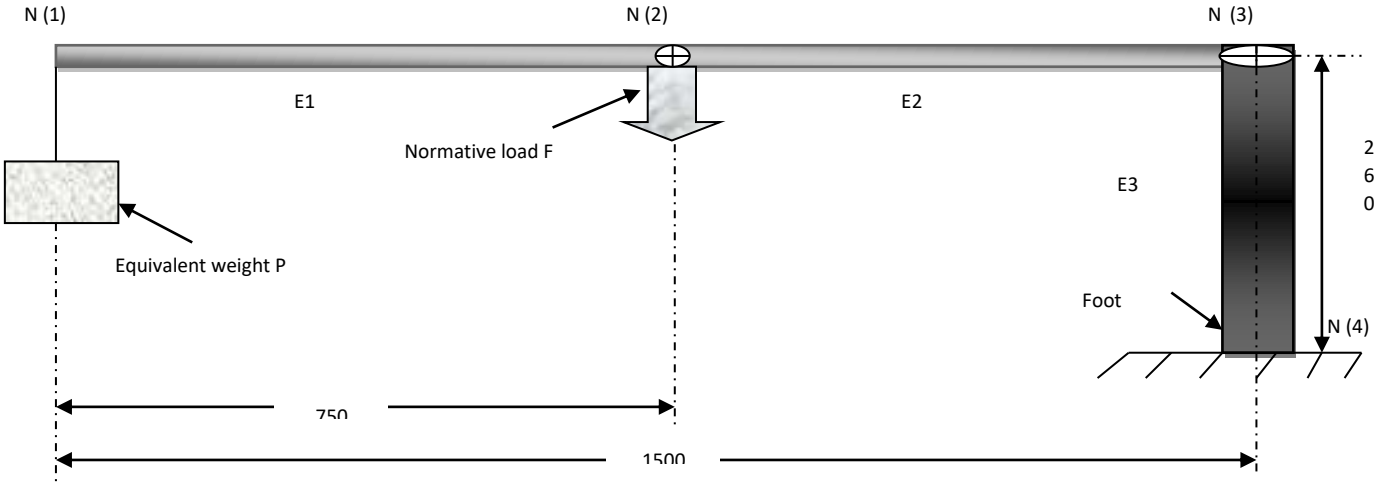

***Figure 4: Diagram of the "3 point" bending resistance test device* [15]**

IJESRT is licensed under a Creative Commons Attribution 4.0 International License.

ISSN: 2277-9655
Impact Factor: 5.164
CODEN: IJESS7

Figure 5*: View of the Experimental device [16]*

For the generalization of the "3 point" bending, the load is not necessarily applied at the centre. The analysis between one end and the point of application of the load is the same, but the problem is no longer symmetrical. When the length of the beam is L and the eccentric load is P, the cutting force is constant in absolute value: it is worth -Pb/L over a length a and + Pa/L over a length b. It changes sign at the point of application of the load P. The bending moment varies linearly between one end, where it is 0, and the point of application of the load P where its absolute value is Pab/L; this is where the risk of rupture is greatest (Figure 6).

A third-degree polynomial describes the profile of the first part of the beam and the arrow is [17]:

$$Y_0 = -\frac{Pb(L^2-b^2)^{\frac{3}{2}}}{9(\sqrt{3}LEI_{gz}} \text{ at point } X_0 = \sqrt{(L^2-b^2)/3} \quad (1)$$

The sharp force diagrams and bending moments are traditionally depicted filled with vertical strokes. This corresponds to the division of trapezoid areas used for the graphical method.

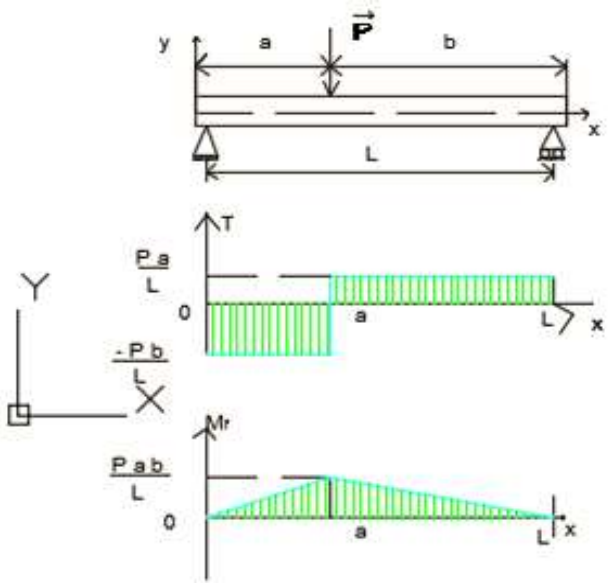

Figure 6*: Three-point bending under an eccentric load*

a. Overview of the behaviour of the flexed tiles

Compared to the beam described above, the thickness of the tile along the Z-axis is relatively small (e = 8 mm) in front of the tile dimensions according to the XY plane (Width l = 25 cm and Length L = 50 cm). The ratio of the smallest of their dimensions to the thickness is equal to 31.25; greater than 20. The tile used is therefore

IJESRT is licensed under a Creative Commons Attribution 4.0 International License.

ISSN: 2277-9655
Impact Factor: 5.164
CODEN: IJESS7

described as a "thin" plate or shell called Kirchhoff [18]. When deflated under appropriate stresses, its mean plane or sheet does not deform at the cutting force but becomes a curved average surface and can have the following two modes of behaviour:

- In XY plane, the so-called “membrane” behaviour or flat state of the stresses;
- In the Z direction, the bending behaviour perpendicular to the mean plane of the tile where displacements from the XY plane are generated.

The actual stresses on plate or shell structures are such that these two modes of behaviour “coexist”. Hence the need to combine the "membrane" and bending properties in the same finite element of the tile [19]. For tile modeling in Robot Structural Analysis (RSA) version 2016, the type of mesh chosen is that of COONS which corresponds well to the rectangular contours. The tiles are discredited into triangular three-node surface finite elements numbered 1, 2 and 3. In the case of purely flexional behaviour, the analysis model uses these surface finite elements with an approximation of the horizontal displacement field U (x,y,z) and V(x,y,z) and vertical W(x,y,z) as follows:

$$\begin{cases} U(x,y,z) = U_0(x,y) + z\theta_x(x,y) \\ V(x,y,z) = V_0(x,y) + z\theta_y(x,y) \\ W(x,y,z) = W_0\,(x,y) \end{cases} \quad (2)$$

$U_0(x,y)$, $V_0(x,y)$ and $W_0\,(x,y)$ are values determined in the mid-thickness average slip. $\theta_x(x,y)$ and $\theta_y(x,y)$ are the two rotations of the section along the X and Y axis. For an inextensible bending plate, the movements of the average sheet in its plane are zero. Therefore: $U_0(x,y) = V_0(x,y) = 0$ and $W_0\,(x,y) \neq 0$. The displacement field becomes:

$$\begin{cases} U(x,y,z) = z\theta_x(x,y) \\ V(x,y,z) = z\theta_y(x,y) \\ W(x,y,z) = W_0\,(x,y) \end{cases} \quad (3)$$

Within the framework of linear elasticity, deformations are expressed as:

$$\begin{cases} \varepsilon_{xx} = \dfrac{\partial U}{\partial x} = z\dfrac{\partial \theta_x}{\partial x} \\ \varepsilon_{yy} = \dfrac{\partial V}{\partial y} = z\dfrac{\partial \theta_y}{\partial y} \\ \varepsilon_{zz} = \dfrac{\partial W}{\partial z} = 0 \\ \varepsilon_{xy} = \dfrac{1}{2}\left(\dfrac{\partial U}{\partial x} + \dfrac{\partial V}{\partial y}\right) = z\left(\dfrac{\partial \theta_x}{\partial y} + \dfrac{\partial \theta_y}{\partial x}\right) \\ \varepsilon_{xz} = \dfrac{1}{2}\left(\dfrac{\partial U}{\partial z} + \dfrac{\partial W}{\partial x}\right) = \theta_x + \dfrac{\partial W_0}{\partial x} \\ \varepsilon_{yz} = \dfrac{1}{2}\left(\dfrac{\partial V}{\partial z} + \dfrac{\partial W}{\partial y}\right) = \theta_y + \dfrac{\partial W_0}{\partial y} \end{cases} \quad (4)$$

According to Kirchhoff’s theory, a straight section remains flat and perpendicular to the average sheet. We can therefore write for deformations:

$$\begin{cases} \varepsilon_{xz} = 0 \Rightarrow \theta_x + \dfrac{\partial W_0}{\partial x} = 0 \Rightarrow \theta_x = -\dfrac{\partial W_0}{\partial x} \\ \varepsilon_{yz} = 0 \Rightarrow \theta_y + \dfrac{\partial W_0}{\partial y} = 0 \Rightarrow \theta_y = -\dfrac{\partial W_0}{\partial y} \end{cases} \quad (5)$$

IJESRT is licensed under a Creative Commons Attribution 4.0 International License.

ISSN: 2277-9655
Impact Factor: 5.164
CODEN: IJESS7

By substituting (5) in (3), horizontal displacements U and V are expressed as a function of vertical displacement W_0 :

$$\begin{cases} U(x,y,z) = -z\,\dfrac{\partial W_0}{\partial x} \\ V(x,y,z) = -z\,\dfrac{\partial W_0}{\partial y} \\ W(x,y,z) = W_0\,(x,y) \end{cases}$$

According to the relationship (5), deformations are written:

$$\begin{cases} \varepsilon_{xx} = \dfrac{\partial U}{\partial x} = z\dfrac{\partial \theta_x}{\partial x} = -z\dfrac{\partial^2 W_0}{\partial x^2} \\ \varepsilon_{yy} = \dfrac{\partial V}{\partial y} = z\dfrac{\partial \theta_y}{\partial y} = -z\dfrac{\partial^2 W_0}{\partial y^2} \\ \varepsilon_{zz} = 0 \\ \varepsilon_{xy} = \dfrac{1}{2}\left(\dfrac{\partial U}{\partial x} + \dfrac{\partial V}{\partial y}\right) = z\left(\dfrac{\partial \theta_x}{\partial y} + \dfrac{\partial \theta_y}{\partial x}\right) = -z\dfrac{\partial^2 W_0}{\partial x\,\partial y} \\ \varepsilon_{xz} = 0 \\ \varepsilon_{yz} = 0 \end{cases}$$

(6)

The deformation state of the plate can therefore be fully described by W_0 (x,y), transverse displacement of the average sheet, and its derivatives. In particular, the thickness is small enough that a linear variation of flat deformations along the normal to the average sheet can be assumed. In order for the plate to remain continuous and not to crease, it is necessary to impose not only the continuity of this transverse displacement but also of its derivative around the edge.

2.5 Expression of the matrix [N (x, y)] of the interpolation functions

The simplest approach to describe the behaviour of a finite element is to approximate its internal displacement field by series of polynomials in order to avoid the violation of the inter-continuity criterion elements that result in physically inadmissible deformation modes for a continuous structure. For the determination of the interpolation functions of the triangular finite element 3 knots, we limit ourselves here to the kinematic theory of Kirchhoff because we especially want to have the continuity of the slope along the edges. In our case, for example, we can write:

$$W_0(x,y) = a_1 + a_2x + a_3y + a_4xy + a_5x^2 + a_6y^2 + a_7x^3 + a_8x^2y + a_9xy^2 + a_{10}y^3 =$$
$$\{1 \quad x \quad y \quad xy \quad x^2 \quad y^2 \quad x^3 \quad x^2y \quad xy^2 \quad y^3\} \; x \; \{a_1 \quad a_2 \quad a_3 \quad a_4 \quad a_5 \quad a_6 \quad a_7 \quad a_8 \quad a_9 \quad a_{10}\}^T$$

(7)

In each node, we take as nodal parameters or connectors the transverse displacements W_i and the two rotations θ_{xi} and θ_{yi} with i = 1, 2, 3 which are the two first derivatives of W_0. With this third degree development for the 3-node triangle, there are 10 generalized internal or co-ordinate variables a_j for 9 external variables or Wi connectors, θ_{xi} and θ_{yi}. The connection matrix [R] connecting connectors to internal variables must be 9 x 9 square. To limit the number of internal variables to 9, one possibility is to assume equal coefficients a8 and a9 [20]. Thus, the relationship (7) is rewritten:

$$W_0(x,y) = a_1 + a_2x + a_3y + a_4xy + a_5x^2 + a_6y^2 + a_7x^3 + a_8(x^2y + xy^2) + a_9y^3 =$$
$$\{1 \quad x \quad y \quad xy \quad x^2 \quad y^2 \quad x^3 \quad x^2y + xy^2 \quad y^3\} \; x \; \{a_1 \quad a_2 \quad a_3 \quad a_4 \quad a_5 \quad a_6 \quad a_7 \quad a_8 \quad a_9\}$$

(8)

From the conditions at the boundary of the $W_0\,(0,0) = W_1$, $\theta_x(0,0) = \theta_{x1}$, $\theta_y(0,0) = \theta_{y1}$ etc., the nodal displacement vector is written:

IJESRT is licensed under a Creative Commons Attribution 4.0 International License.

ISSN: 2277-9655
Impact Factor: 5.164
CODEN: IJESS7

$$\begin{Bmatrix} W_1 \\ \theta_{x1} \\ \theta_{y1} \\ W_2 \\ \theta_{x2} \\ \theta_{y2} \\ W_3 \\ \theta_{x3} \\ \theta_{y3} \end{Bmatrix} = [R]\ X \begin{Bmatrix} a_1 \\ a_2 \\ a_3 \\ a_4 \\ a_5 \\ a_6 \\ a_7 \\ a_8 \\ a_9 \end{Bmatrix}$$

(9)

The connection matrix [R] is written:

$$[R] = \begin{bmatrix} 1 & 0 & 0 & 0 & 0 & 0 & & 0 & 0 & 0 & \\ 0 & 1 & 0 & 0 & 0 & 0 & & 0 & 0 & 0 & \\ 0 & 0 & 1 & 0 & 0 & 0 & & 0 & 0 & 0 & \\ 1 & x_2 & y_2 & x_2y_2 & x_2^2 & y_2^2 & x_2^3 & x_2^3y_2 + x_2y_2^3 & & y_2^3 \\ 0 & 1 & 0 & y_2 & 2x_2 & 0 & 3x_2^2 & 3x_2^2y_2 + y_2^3 & & 0 \\ 0 & 0 & 1 & x_2 & 0 & 2y_2 & 0 & x_2^3 + 3x_2y_2^2 & & 3y_2^2 \\ 1 & x_3 & y_3 & x_3y_3 & x_3^2 & y_3^2 & x_3^3 & x_3^3y_3 + x_3y_3^3 & & y_3^3 \\ 0 & 1 & 0 & y_3 & 2x_3 & 0 & 3x_3^2 & 3x_3^2y_3 + y_3^3 & & 0 \\ 0 & 0 & 1 & x_3 & 0 & 2y_3 & 0 & x_3^3 + 3x_3y_3^2 & & 3y_3^2 \end{bmatrix}$$

By injecting (9) into (8), we have:

$W_0(x,y) = \{1 \quad x \quad y \quad xy \quad x^2 \quad y^2 \quad x^3 \quad x^2y + xy^2 \quad y^3\}$ x $[R]^{-1}$
x$\{w_1 \quad \theta_{x1} \quad \theta_{y1} \quad W_2 \quad \theta_{x2} \quad \theta_{y2} \quad W_3 \quad \theta_{x3} \quad \theta_{y3}\}^T$, où

$$[R]^{-1} = \frac{1}{\Delta} \times \begin{bmatrix} \Delta & 0 & 0 & 0 & 0 & 0 & 0 & 0 & 0 \\ 0 & \Delta & 0 & 0 & 0 & 0 & 0 & 0 & 0 \\ 0 & 0 & \Delta & 0 & 0 & 0 & 0 & 0 & 0 \\ T_{41} & T_{42} & T_{43} & T_{44} & T_{45} & T_{46} & T_{47} & T_{48} & T_{49} \\ T_{51} & T_{52} & T_{53} & T_{54} & T_{55} & T_{56} & T_{57} & T_{58} & T_{59} \\ T_{61} & T_{62} & T_{63} & T_{64} & T_{65} & T_{66} & T_{67} & T_{68} & T_{69} \\ T_{71} & T_{72} & T_{73} & T_{74} & T_{75} & T_{76} & T_{77} & T_{78} & T_{79} \\ T_{81} & T_{82} & T_{83} & T_{84} & T_{85} & T_{86} & T_{87} & T_{88} & T_{89} \\ T_{91} & T_{92} & T_{93} & T_{94} & T_{95} & T_{96} & T_{97} & T_{98} & T_{99} \end{bmatrix}$$

(10)

is the reverse of the R connection matrix as the R^{-1} determinant is defined by:

$\Delta = (x_2y_3 - x_3y_2)^3 \quad (x_2^4y_3^2 \quad -x_2^3y_2y_3x_3 + (-3(y_2 - y_3)^2x_3^2 + 3y_2^2y_3^2 - y_3^4)x_2^2 - x_3y_2y_3(x_3^2 - y_2^2) + 6y_2y_3 - y_3^2)x_2 + x_3^2y_2^2(x_3^2 - y_2^2 + 3y_3^2))$.

(11)

T_{ij} are the terms of R-1: i represent the row and j represents the column of the matrix 9 x 9 (see Appendix).

$W_0(x,y) = [N(x,y)]$ x $\{w_1 \quad \theta_{x1} \quad \theta_{y1} \quad W_2 \quad \theta_{x2} \quad \theta_{y2} \quad W_3 \quad \theta_{x3} \quad \theta_{y3}\}^T$

The matrix of interpolation functions [N(x,y)] is written:

$$[N(x,y)] = \frac{1}{\Delta} x \{\Delta + T_{41}xy + T_{51}x^2 + T_{61}y^2 + T_{71}x^3 + T_{81}(x^2y + xy^2) + T_{91}y^3 \ \Delta x + T_{42}xy + T_{52}x^2 + T_{62}y^2 + T_{72}x^3 + T_{82}(x^2y + xy^2) + T_{92}y^3 \ \Delta y + T_{43}xy + T_{53}x^2 + T_{63}y^2 + T_{73}x^3 + T_{83}(x^2y + xy^2) + T_{93}y^3 \ T_{44}xy + T_{54}x^2 + T_{64}y^2 + T_{74}x^3 + T_{84}(x^2y + xy^2) + T_{94}y^3 \ T_{45}xy + T_{55}x^2 + T_{65}y^2 + T_{75}x^3 + T_{85}(x^2y + xy^2) + T_{95}y^3 \ T_{46}xy + T_{56}x^2 + T_{66}y^2 + T_{76}x^3 + T_{86}(x^2y + xy^2) + T_{96}y^3 \ T_{47}xy + T_{57}x^2 + T_{67}y^2 + T_{77}x^3 + T_{87}(x^2y + xy^2) + T_{97}y^3 \ T_{48}xy + T_{58}x^2 + T_{68}y^2 + T_{78}x^3 + T_{88}(x^2y + xy^2) + T_{98}y^3 \ T_{49}xy + T_{59}x^2 + T_{69}y^2 + T_{79}x^3 + T_{89}(x^2y + xy^2) + T_{99}y^3\}$$

(12)

IJESRT is licensed under a Creative Commons Attribution 4.0 International License.

ISSN: 2277-9655
Impact Factor: 5.164
CODEN: IJESS7

According to the relation (6), the field of deformation becomes:

$\varepsilon_{xx} = [B_1]\ X\ \{w_1\ \ \theta_{x1}\ \ \theta_{y1}\ \ W_2\ \ \theta_{x2}\ \ \theta_{y2}\ \ W_3\ \ \theta_{x3}\ \ \theta_{y3}\}^T$

$[B_1] = -\frac{z}{\Delta}\ x\ \{\ 2T_{51} + 6T_{71}x + 2T_{81}y\ \ 2T_{52} + 6T_{72}x + 2T_{82}y\ \ 2T_{53} + 6T_{73}x + 2T_{83}y\ \ 2T_{54} + 6T_{74}x + 2T_{84}y\ \ + 2T_{55} + 6T_{75}x + 2T_{85}y\ \ 2T_{56} + 6T_{76}x + 2T_{86}y\ \ 2\,T_{57} + 6T_{77}x + 2T_{87}y\ \ 2T_{58} + 6T_{78}x + 2T_{88}y)\ \ 2T_{59} + 6T_{79}x + 2T_{89}y\}$

$\varepsilon_{yy} = [B_2]\ X\ \{w_1\ \ \theta_{x1}\ \ \theta_{y1}\ \ W_2\ \ \theta_{x2}\ \ \theta_{y2}\ \ W_3\ \ \theta_{x3}\ \ \theta_{y3}\}^T$

$[B_2] = -\frac{z}{\Delta}\ x\ \{\ 2T_{61} + 2T_{81}x + 6T_{91}y\ \ 2T_{82}x + (2T_{62} + 6T_{92})y\ \ 2T_{63} + 2T_{83}x + 6T_{93}y\ \ 2T_{64} + 2T_{84}x + 6T_{94}y\ \ 2T_{65} + 2T_{85}x + 6T_{95}y\ \ T_{86}x + (2T_{66} + 6T_{96})y\ \ 2T_{67} + 2T_{87}x + 6T_{97}y\ \ 2T_{68} + 2T_{88}x + 6T_{98}y\ \ 2T_{69} + 2T_{89}x + 6T_{99}y\}$

$\varepsilon = [B] = \begin{bmatrix} B_1 \\ B_2 \end{bmatrix}\ x\ \ \{w_1\ \ \theta_{x1}\ \ \theta_{y1}\ \ W_2\ \ \theta_{x2}\ \ \theta_{y2}\ \ W_3\ \ \theta_{x3}\ \ \theta_{y3}\}^T$ (13)

2.6 Expression of the rigidity matrix $[K]^{él.}$ of the triangular finite element 3 knots

The conventional method based on the interpolation functions developed in the preceding paragraph is used for the generation of the elementary matrix $[K]^{él.}$ of "stiffness" of the triangular finite element at 3 knots that is written [20]:

$[K]^{él.} = \int [B]^T [H].[B].dv$ (14)

[B] is the matrix that connects the deformation field to the nodal displacements and dv = dxdy. e an elementary volume

After the constitution of the overall matrix of the structure $[K]^{Str.}$ by assembling the elementary matrices $[K]^{el.}$ expressed in the global benchmark, the complete system expressing the behaviour at the static equilibrium of the tile is written:

$\{F\} = [K]^{Str.}.\{U\}$ (15)

{F}: Vector representing external forces applied to the tile
{U}: Vector representing the nodal displacement field

The relation (14) constitutes a system of linear equations whose unknowns are the nodal displacements or degrees of freedom and the actions of links or reactions of supports. The Skyline resolution method implemented in the Autodesk Robot Structural Analysis Professional 2016 software seems the best solution for this system. In fact, the shapes of the tiles and their type of mesh by three-knot triangular finite elements are simple so do not require huge machine resources. Also, to make it impossible to move the whole tile, it is necessary to support it properly.

By means of the relationships (16)-(20), it is possible to determine and exploit the different results of the displacement fields, stresses and deformations in the tiles according to their disturbances.

2.7 Moments relationships – Curvatures

The three relationships between M_x, M_y and M_{xy} moments and curvatures χ_x, χ_y et χ_{xy} can be grouped within a matrix expression where the flexural rigidity D of the tile appears, similar to the EI product of bending beam theory. The inverse relations connecting the curvatures to the moments give the shape that the average sheet takes when applied to it the moments.

$$\begin{Bmatrix} M_x \\ M_y \\ M_z \end{Bmatrix} = \frac{Ee^2}{12(1-\nu^2)} \begin{bmatrix} 1 & \nu & 0 \\ \nu & 1 & 0 \\ 0 & 0 & \frac{1-\nu}{2} \end{bmatrix} \begin{Bmatrix} \chi_x \\ \chi_y \\ \chi_{xy} \end{Bmatrix} \qquad D = \frac{Ee^2}{12(1-\nu^2)}$$

(16)

IJESRT is licensed under a Creative Commons Attribution 4.0 International License.

ISSN: 2277-9655
Impact Factor: 5.164
CODEN: IJESS7

2.8 Stress Relationships – Moments

Similarly, normal and shear stresses can be connected to the bending and twisting moments by:

$$\sigma_{xx} = \frac{12z.M_{xx}}{e^3} \qquad \sigma_{yy} = \frac{12z.M_{yy}}{e^3} \qquad \sigma_{xy} = \frac{12z.M_{xy}}{e^3} \tag{17}$$

This gives for the extreme fibers of the tile $e = \pm \frac{e}{2}$ where the extreme values of normal and tangential stresses:

$$\sigma_{xx} = \pm\frac{6M_{xx}}{e^2} \qquad \sigma_{yy} = \pm\frac{6M_{yy}}{e^2} \qquad \sigma_{xy} = \pm\frac{6M_{xy}}{e^2} \tag{18}$$

2.9 Stress - deformation relationships

In the case of an isotropic material, Hooke's law states:

$$\sigma_{ij} = \frac{E}{1+\upsilon}\left(\varepsilon_{ij} + \frac{\nu}{1-2\nu}\,\varepsilon_{kk}\delta_{ij}\right) \tag{19}$$

- δ_{ij} the Kronecker symbol equal to 1 if i = j and 0 if $i \neq j$
- ε_{kk} the trace of the tensor of the deformations (sum of the diagonal terms of the tensor).

Relationships (19) can be reversed to give relationships (20) :

$$\epsilon_{ij} = \frac{1}{E}\left[(1+\nu)\sigma_{ij} - \nu\sigma_{kk}\delta_{ij}\right] \tag{20}$$

3. RESULTS AND DISCUSSIONS

According to the conditions at the limits mentioned above, we apply a normative load F to each type of tile. The physical quantities involved in the study of the behaviour of the flexed tiles are:

- The vertical displacement field W_0 on the Z axis;
- The rotation field $\theta_x = R_{xx}$ or $\theta_y = R_{yy}$;
- Normal stress fields σ_{xx} and σ_{yy} and strain fields ϵ_{xx} and ϵ_{yy}.

To complete the discussions, the following approach will be taken:

- Comparison of the relevant values of the physical quantities with the permissible values recommended by the EN 1992 rules: Concrete structures (EC2);
- Comparison of results for different types of tiles;
- Analysis and interpretation of the results of the comparison.

By convention, relative elongation and tensile stresses are positive while relative shortening and compressive stresses are negative. The checks are performed at the service limit states (SLE) related to tile operation and the ultimate limit states (ULS) related to the bearing capacity of the tile.

SLE: Concrete compression is limited to 0.6 f28 = 0.6 x 20 = 12 MPa and the allowable deflection of the tile is limited to l/500 = 370/500 = 0.74 mm.
ULS: The deformation (relative shortening) of the bending concrete is limited to: 3, 5‰.

IJESRT is licensed under a Creative Commons Attribution 4.0 International License.

ISSN: 2277-9655
Impact Factor: 5.164
CODEN: IJESS7

3.1 Vertical Displacement W and Rotation Fields R_{xx}

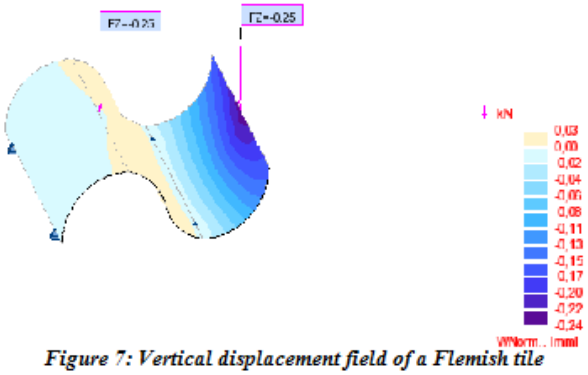

Figure 7: Vertical displacement field of a Flemish tile

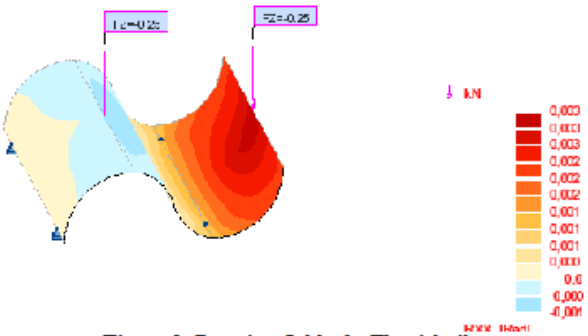

Figure 8: Rotation field of a Flemish tile

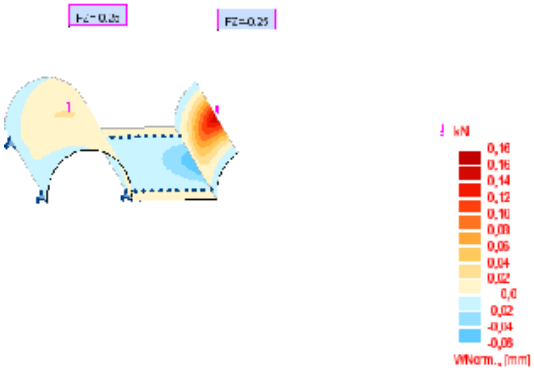

Figure 9: Vertical displacement field of a Romanesque tile

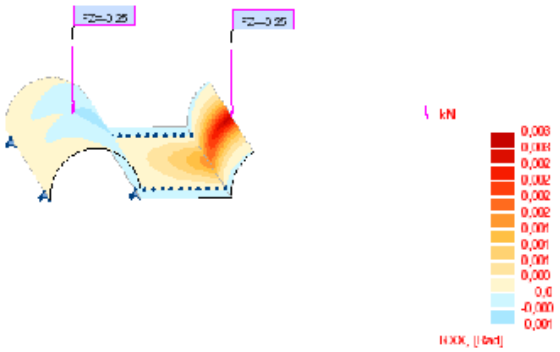

Figure 10: Rotation field of a Romanesque tile

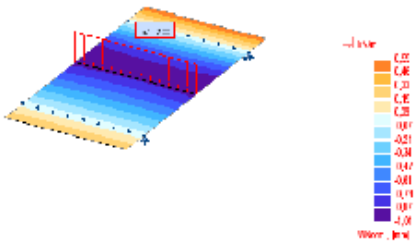

Figure 11: Vertical displacement field of a Flat tile

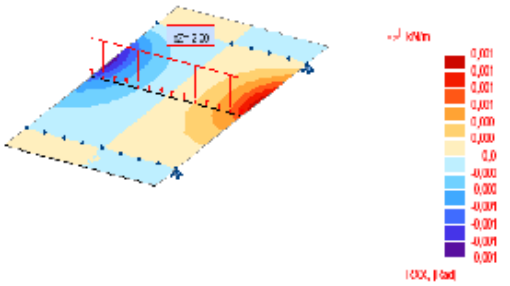

Figure 12: Rotation field of a Flat tile

IJESRT is licensed under a Creative Commons Attribution 4.0 International License.

ISSN: 2277-9655
Impact Factor: 5.164
CODEN: IJESS7

3.2 Normal constraint Fields σ_{xx} et σ_{yy}

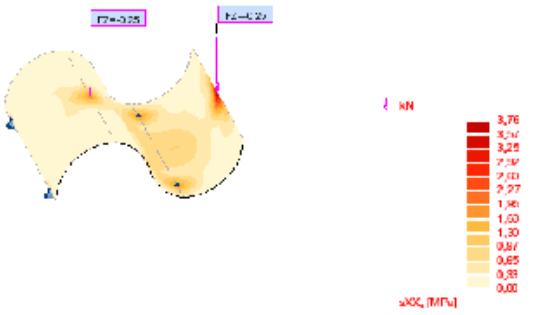

Figure 13: Normal constraint field σ_{xx} of a Flemish tile

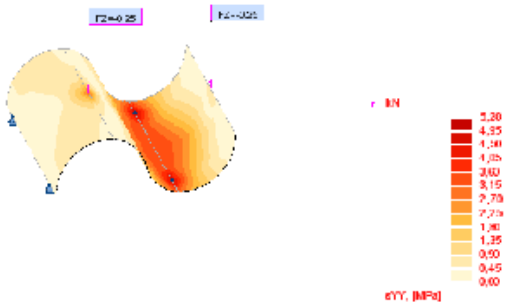

Figure 14: Normal constraint field σ_{yy} of a Flemish tile

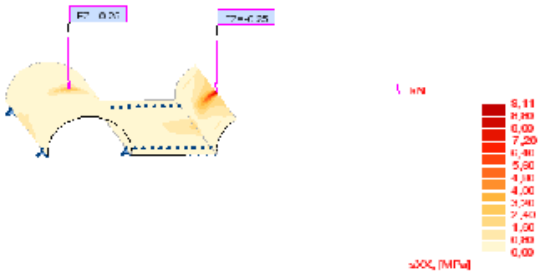

Figure 15: Normal constraint field σ_{xx} of a Romanesque tile

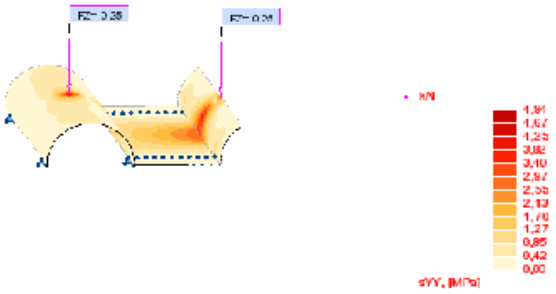

Figure 16: Normal constraint field σ_{yy} of a Romanesque tile

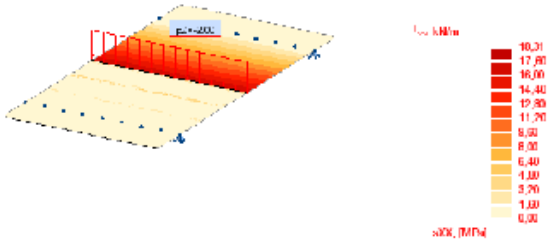

Figure 17: Normal constraint field σ_{xx} of a Flat tile

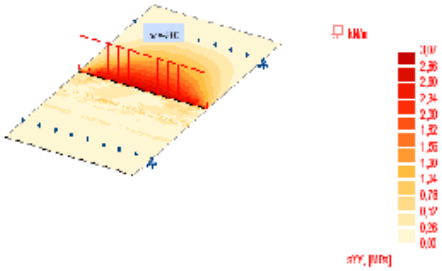

Figure 18: Normal constraint field σ_{yy} of a Flat tile

Table 2: Summary of normal stress and strain results, Arrows and Rotations

Tile	σ_{xx} (MPa)	σ_{yy} (MPa)	ε_{xx} (‰)	ε_{yy} (‰)	W (mm)	R_{xx} (Rd)	R_{yy} (Rd)
Flemish	3,28	5,94	0,1	0,2	0,24	0,003	0,000
Romanesque	9,11	4,94	0,3	0,1	0,16	0,003	0,001
Flat	18,31	3,07	0,6	0,0	1,01	0,001	0,010

The deformation results presented in Table 2 show that for a normative load of 50 kg, all three tile shapes have a good bearing capacity because the bending deformations in the tiles are less than the limit deformation of the concrete which is 3,5‰. However, the Plate tile bears less than the Romanesque and Flemish tiles. For normal operating conditions and in-service durability aspects, the concrete compression limit stress (12MPa) and limit

IJESRT is licensed under a Creative Commons Attribution 4.0 International License.

ISSN: 2277-9655
Impact Factor: 5.164
CODEN: IJESS7

deflection (0.74 mm) are significantly exceeded for the Flat tile. The Flemish tile seems to offer a little more of the best operating conditions and durability in service than the Romanesque tile.

The validation of the numerical results is made by comparison with the experimental results of the tests carried out on the flat tile. The tile is placed on the supports of the experimental device in Figure 5. The normative load F is applied in the middle of the tile. A BORLEETI comparator (0.01 mm 0 - 10 mm) placed under and in the middle of the tile records the arrow W (mm). For a normative load F = 2 kN/m, one finds by experiment approximately the value of the digital arrow W = 1.01 mm. By experiment, when the load F is gradually increased, the arrow increases linearly: which is consistent with the type of numerical analysis considered. For a value of F = 12 kN/m, the numeric value of the arrow is 6.05 mm and the calculated normal stress values are σ_{xx} = 110.97 MPa and σ_{yy} = 18.44 MPa. The maximum deformation is ε = 3.6‰, a value greater than the limit deformation of the bending concrete (3.5‰) which is assimilated to the break of the flat tile. When the load of 12 kN/m is repeated, a sharp break of the tile is observed. From this observation, the numerical method explained in this study also makes it possible to predict the carrying capacity of a tile, hence its validity.

4. CONCLUSION

The results obtained show that in relation to the flat shape, the concave and or convex shapes have an influence on the behaviour of a tile loaded in bending. Their presence results in a sharp decrease of the arrow, normal stresses and deformations in the direction of the smallest span of the tile (width) and a small increase in normal stresses and deformations in the direction of maximum reach (length). Based on this observation, the load-bearing capacity of a Flemish tile is significantly higher than that of a Romanesque tile because of the presence of the flat part in the Romanesque tile. Therefore, this study recommends that the tile manufacturer be very careful about the mechanical characteristics of the materials used in tile production. The values of these characteristics must be higher for flat tiles if the same results as Flemish or Romanesque tiles are to be obtained.

APPENDIX

$$T_{41} = 6(x_2 - x_3)(y_2 - y_3)(2x_2^4x_3y_2^2y_3 - x_2^4x_3y_2y_3^2 - x_2^4x_3y_3^3 - 3x_2^3x_3^2y_2^2y_3 + 3x_2^3x_3^2y_2y_3^2 + x_2^3y_2y_3^4 - 3x_2^2x_3^3y_2^2y_3 + 3x_2^2x_3^3y_2y_3^2 + 2x_2^2x_3y_2^4y_3 - 3x_2^2x_3y_2^3y_3^2 - 3x_2^2x_3y_2^2y_3^3 + x_2^2x_3y_2y_3^4 + x_2x_3^4y_2^3 + x_2x_3^4y_2^2y_3 - 2x_2x_3^4y_2y_3^2 - x_2x_3^2y_2^4y_3 + 3x_2x_3^2y_2^3y_3^2y_3 + 3x_2x_3^2y_2^2y_3^3y_3 - 2x_2x_3^2y_2y_3^4 - x_3^3y_2^4y_3)$$

$$T_{42} = -(x_2 - x_3)(x_2^6y_3^4 - 3x_2^5x_3y_3^4 - 6x_2^4x_3^2y_2^3y_3 + 9x_2^4x_3^2y_2^2y_3^2 + 3x_2^4y_2^2y_3^4 + 14x_2^3x_3^3y_2^3y_3 - 30x_2^3x_3^3y_2^2y_3^2 + 14x_2^3x_3^3y_2y_3^3 - 18x_2^3x_3y_2^2y_3^4 + 6x_2^3x_3y_2y_3^5 + 9x_2^2x_3^4y_2^2y_3^2 - 6x_2^2x_3^4y_2y_3^3 - 6x_2^2x_3^2y_2^5y_3 + 15x_2^2x_3^2y_2^4y_3^2 + 15x_2^2x_3^2y_2^2y_3^4 - 6x_2^2x_3^2y_2y_3^5 - 3x_2x_3^5y_2^4 + 6x_2x_3^3y_2^5y_3 - 18x_2x_3^3y_2^4y_3^2 + x_3^6y_2^4 + 3x_3^4y_2^4y_3^2)$$

$$T_{43} = (y_2 - y_3)(6x_2^5x_3y_2^2y_3^2 - 6x_2^5x_3y_2y_3^3 - 15x_2^4x_3^2y_2^2y_3^2 + 18x_2^4x_3^2y_2y_3^3 - 3x_2^4x_3^2y_3^4 + 3x_2^4y_2y_3^5 - x_2^4y_3^6 + 6x_2^3x_3y_2^4y_3^2 - 14x_2^3x_3y_2^3y_3^3 - 3x_2^2x_3^4y_2^4 + 18x_2^2x_3^2y_2^3y_3 - 15x_2^2x_3^4y_2^2y_3^2 - 9x_2^2x_3^2y_2^4y_3^2 + 30x_2^2x_3^2y_2^3y_3^3 - 9x_2^2x_3^2y_2^2y_3^4 - 6x_2x_3^5y_2^3y_3 + 6x_2x_3^5y_2^2y_3^2 - 14x_2x_3^3y_2^3y_3^3 + 6x_2x_3^3y_2^2y_3^4 - x_3^4y_2^6 + 3x_3^4y_2^5y_3)$$

$$T_{44} = -6x_3y_3(x_2^5y_3^3 - x_2^4x_3y_3^3 + 3x_2^3y_2^2y_3^3 + 3x_2^2x_3^3y_2^3 - 9x_2^2x_3^3y_2^2y_3 + 5x_2^2x_3^3y_2y_3^2 - 9x_2^2x_3y_2^2y_3^3 + 3x_2^2x_3y_2y_3^4 + 3x_2x_3^4y_2^2y_3 - 2x_2x_3^4y_2y_3^2 + 5x_2x_3^2y_2^2y_3^3 - 2x_2x_3^2y_2y_3^4 + x_3^3y_2^5 - x_3^3y_2^4y_3)$$

$$T_{45} = x_3(2x_2^6y_3^4 - 3x_2^5x_3y_3^4 + 6x_2^4y_2^2y_3^4 + 4x_2^3x_3^3y_2^3y_3 - 15x_2^3x_3^3y_2^2y_3^2 + 10x_2^3x_3^3y_2y_3^3 - 21x_2^3x_3y_2^2y_3^4 + 6x_2^3x_3y_2y_3^5 + 9x_2^2x_3^4y_2^2y_3^2 - 6x_2^2x_3^4y_2y_3^3 + 15x_2^2x_3^2y_2^2y_3^4 - 6x_2^2x_3^2y_2y_3^5 + 3x_2x_3^3y_2^4y_3^2 - x_3^6y_2^4 - 3x_3^4y_2^4y_3^2)$$

$$T_{46} = y_3(2x_3^4y_2^6 - 3x_3^4y_2^5y_3 + 3x_2^4x_3^2y_2y_3^3 + 4x_2^3x_3y_2^3y_3^3 - 15x_2^2x_3^2y_2^3y_3^3 + 10x_2x_3^3y_2^3y_3^3 - 21x_2^2x_3^4y_2^3y_3 + 6x_2^2x_3^4y_2^4 + 9x_2^2x_3^2y_2^2y_3^4 - 6x_2x_3^3y_2^2y_3^4 + 15x_2^2x_3^4y_2^2y_3^2 - 6x_2x_3^5y_2^2y_3^2 - 3x_2^4x_3^2y_3^4 - x_2^4y_3^6 + 6x_2x_3^5y_2^3y_3)$$

$$T_{47} = -6x_2y_2(2x_2^4x_3y_2^2y_3 - 3x_2^4x_3y_2y_3^2 - 5x_2^3x_3^2y_2^2y_3 + 9x_2^3x_3^2y_2y_3^2 - 3x_2^3x_3^2y_3^3 + x_2^3y_2y_3^4 - 5x_2^2x_3y_2^3y_3^2 + 2x_2^2x_3y_2^4y_3 - 3x_2x_3^2y_2^4y_3 + 9x_2x_3^2y_2^3y_3^2 + x_2x_3^4y_2^3 - x_2^3y_3^5 - x_3^5y_2^3 - 3x_3^3y_2^3y_3^2)$$

$$T_{48} = x_2(x_2^6y_3^4 + 6x_2^4x_3^2y_2^3y_3 - 9x_2^4x_3^2y_2^2y_3^2 + 3x_2^4y_2^2y_3^4 - 10x_2^3x_3^3y_2^3y_3 + 15x_2^3x_3^3y_2^2y_3^2 - 4x_2^3x_3^3y_2y_3^3 - 3x_2^3x_3y_2^2y_3^4 + 6x_2^2x_3^2y_2^5y_3 - 15x_2^2x_3^2y_2^4y_3^2 + 3x_2x_3^5y_2^4 - 6x_2x_3^3y_2^5y_3 + 21x_2x_3^3y_2^4y_3^2 - 2x_3^6y_2^4 - 6x_3^4y_2^4y_3^2)$$

IJESRT is licensed under a Creative Commons Attribution 4.0 International License.

ISSN: 2277-9655
Impact Factor: 5.164
CODEN: IJESS7

$$T_{49} = y_2(6x_2^5x_3y_2^2y_3^2 - 6x_2^3x_3y_2y_3^3 - 15x_2^4x_3^2y_2^2y_3^2 - 10x_2^3x_3y_2^3y_3^3 + 21x_2^4x_3^2y_2y_3^3 - 6x_2^4x_3^3y_3^4 + 3x_2^4y_2y_3^5 - 2x_2^4y_3^6 - 9x_2^2x_3^2y_2^2y_3^4 + 6x_2^3x_3y_2^2y_3^3 + 15x_2^2x_3^2y_2^3y_3^3 - 6x_2x_3^5y_2^2y_3^2 + 3x_2^2x_3^4y_2^4 - 4x_2x_3^3y_2^3y_3^3 + x_3^4y_2^6)$$

$$T_{51} = -3(y_2 - y_3)^2(2x_2^5y_2y_3^2 + x_2^5y_3^3 - 8x_2^3x_3^2y_2^2y_3^3 - 4x_2^3x_3^2y_2y_3^2 - 3x_2^3x_3^2y_3^3 + 2x_2^3y_2^3y_3^2 - x_2^3y_2^2y_3^3 - 2x_2^3y_2y_3^4 - x_2^3y_3^5 + 3x_2^2x_3^3y_2^3 + 4x_2^2x_3^3y_2^2y_3 + 8x_2^2x_3^3y_2y_3^2y_3 + 2x_2^2x_3y_2^2y_3^3 + 4x_2^2x_3y_2y_3^4 - 4x_2x_3^2y_2^4y_3 - 2x_2x_3^2y_2^3y_3^2 - x_3^5y_2^3 - 2x_3^5y_2^2y_3 + x_3^3y_2^5 + 2x_3^3y_2^4y_3 + x_3^3y_2^3y_3^2 - 2x_3^3y_2^2y_3^3$$

$$T_{52} = (y_2 - y_3)(2x_2^6y_3^4 - 3x_2^5x_3y_2^2y_3^2 - 6x_2^4x_3^2y_3^4 + 4x_2^4y_2^2y_3^4 - 2x_2^4y_2y_3^5 - 2x_2^4y_3^6 + 16x_2^3x_3^3y_2^3y_3 - 18x_2^3x_3^3y_2^2y_3^2 + 16x_2^3x_3^3y_2y_3^3 - 3x_2^3x_3y_2^4y_3^2 + 2x_2^3x_3y_2^3y_3^3 - 7x_2^3x_3y_2^2y_3^4 + 3x_2^4y_2y_3^5 + 6x_2^3x_3y_2^4y_3^2 - 14x_2^3x_3y_2^3y_3^3 - 3x_2^2x_3^4y_2^4 - 15x_2^3x_3^3y_2^2y_3^2 - 9x_2^2x_3^2y_2^4y_3^2 + 30x_2^2x_3^3y_2^3y_3^3 - 9x_2^2x_3^2y_2^2y_3^4 - 6x_2x_3^5y_2^3y_3 + 6x_2x_3^5y_2^2y_3^2 - 14x_2x_3^3y_2^3y_3^3 + 6x_2x_3^3y_2^3y_3^4 - x_3^4y_2^6 + 3x_3^4y_2^5y_3)$$

$$T_{53} = -y_2y_3(y_2 - y_3)^2(3x_2^5y_3^2 - 12x_2^3x_3^2y_2y_3 - 3x_2^3x_3^2y_3^2 + 3x_2^3y_2^2y_3^2 - 4x_2^3y_2y_3^3 - x_2^3y_3^4 + 3x_2^2x_3^3y_2^2 + 12x_2^2x_3^3y_2y_3 + 6x_2^2x_3y_2y_3^3 - 6x_2x_3^2y_2^3y_3 - 3x_3^5y_2^2 + x_3^3y_2^4 + 4x_3^3y_2^3y_3 - 3x_3^3y_2^2y_3^2)$$

$$T_{54} = 3y_3^2(x_2^5y_3^2 + 2x_2^3x_3^2y_3^2 - 3x_2^3x_3^2y_3^3 + 3x_2^3y_2^2y_3^3 - x_2^3y_3^5 + 3x_2^2x_3^3y_3^2 - 12x_2^2x_3^3y_2^2y_3 + 8x_2^2x_3^3y_2y_3^2 - 6x_2^2x_3y_2^2y_3^3 + 4x_2^2x_3y_2y_3^4 - 2x_2x_3^2y_2^3y_3^2 + 3x_3^5y_2^2 - 2x_3^5y_2^2y_3 + x_3^3y_2^5 - 2x_3^3y_2^4y_3 + 5x_3^3y_2^3y_3^2 - 2x_3^3y_2^2y_3^3)$$

$$T_{55} = -y_3(x_2^6y_3^4 - 3x_2^4x_3^2y_3^4 + 3x_2^4y_2^2y_3^4 - x_2^4y_3^6 + 2x_2^3x_3^3y_2^3y_3 - 9x_2^3x_3^3y_2^2y_3^2 + 8x_2^3x_3^3y_2y_3^3 - 6x_2^3x_3y_2^2y_3^4 + 4x_2^3x_3y_2y_3^5 - 6x_2^2x_3^2y_2^3y_3^3 + 6x_2x_3^5y_2^3y_3 - 3x_2x_3^5y_2^2y_3^2 + 10x_2x_3^3y_2^3y_3^3 - 3x_2x_3^3y_2^2y_3^4 - 2x_3^6y_2^4 - 4x_3^4y_2^4y_3^2)$$

$$T_{56} = -y_2y_3(y_2 - y_3)(6x_2^3x_3^2y_3^2 + 2x_2^3y_2y_3^3 + 2x_2^3y_3^4 + 3x_2^2x_3^3y_2^2 - 12x_2^2x_3^3y_2y_3 - 6x_2^2x_3y_2y_3^3 + 3x_3^5y_2^2 + x_2^3y_3^4 - 2x_3^3y_2^3y_3 + 3x_3^3y_2^2y_3^2)$$

$$T_{57} = 3y_2^2(2x_2^5y_2y_3^2 - 3x_2^5y_3^3 - 8x_2^3x_3^2y_2^2y_3 + 12x_2^3x_3^2y_2y_3^2 - 3x_2^3x_3^2y_3^3 + 2x_2^3y_2^3y_3^2 - 5x_2^3y_2^2y_3^3 + 2x_2^3y_2y_3^4 - x_2^3y_3^5 + 3x_2^2x_3^3y_2^3 - 2x_2^2x_3^3y_2^2y_3 + 2x_2^2x_3y_2^2y_3^3 - 4x_2x_3^2y_2^4y_3 + 6x_2x_3^2y_2^3y_3^2 - x_3^5y_2^3 + x_3^3y_2^5 - 3x_3^3y_2^3y_3^2)$$

$$T_{58} = -y_2(2x_2^6y_3^4 + 3x_2^5x_3y_2^2y_3^2 - 6x_2^5x_3y_2y_3^3 + 4x_2^4y_2^2y_3^4 - 8x_2^3x_3^3y_2^3y_3 + 9x_2^3x_3^3y_2^2y_3^2 - 2x_2^3x_3^3y_2y_3^3 + 3x_2^3x_3y_2^4y_3^2 - 10x_2^3x_3y_2^3y_3^3 - 3x_2^2x_3^3y_2^2y_3^4 + 3x_2^2x_3^4y_2^4 + 6x_2^2x_3^2y_2^3y_3^3 - 4x_2x_3^3y_2^5y_3 + 6x_2x_3^3y_2^4y_3^2 - x_3^6y_2^4 + x_3^4y_2^6 - 3x_3^4y_2^4y_3^2)$$

$$T_{59} = -y_3(y_2 - y_3)(3x_2^5y_3^2 - 12x_2^3x_3^2y_2y_3 + 3x_2^3x_3^2y_3^2 + 3x_2^3y_2^2y_3^2 - 2x_2^3y_2y_3^3 + x_2^3y_3^4 + 6x_2^2x_3^3y_2^2 - 6x_2x_3^2y_2^3y_3 + 2x_3^3y_2^4 + 2x_3^3y_2^3y_3)$$

$$T_{61} = -3(x_2 - x_3)^2(x_2^5y_3^3 - 4x_2^4x_3y_2y_3^2 + 2x_2^4x_3y_3^3 + 2x_2^3x_3^2y_2^2 - 2x_2^3x_3^2y_2y_3^2 + x_2^3x_3^2y_3^3 + 3x_2^3y_2^2y_3^3 - x_2^3y_3^5 - x_2^2x_3^3y_3^3 + 2x_2^2x_3^3y_2^2y_3 - 2x_2^2x_3^3y_3^3 - 8x_2^2x_3y_2^3y_3^2 + 4x_2^2x_3y_2^2y_3^3 - 2x_2^2x_3y_3^5 - 2x_2x_3^4y_2^3 + 4x_2x_3^4y_2^2y_3 + 2x_2x_3^2y_2^4 - 4x_2x_3^2y_2^3y_3^2 + 8x_2x_3^2y_2^2y_3^3 - x_3^5y_2^3 + x_3^3y_2^5 - 3x_3^3y_2^3y_3^2)$$

$$T_{62} = -x_2x_3(x_2 - x_3)^2(x_2^4y_3^3 - 6x_2^3x_3y_2y_3^2 + 4x_2^3x_3y_3^3 + 3x_2^2x_3^2y_2^2 - 3x_2^2x_3^2y_3^3 + 3x_2^2y_2^2y_3^3 - 3x_2^2y_3^5 - 4x_2x_3^3y_2^3 + 6x_2x_3^3y_2^2y_3 - 12x_2x_3^3y_2y_3^2 + 12x_2x_3y_2^2y_3^3 - x_3^4y_2^5 + 3x_3^2y_2^5 - 3x_3^2y_2^3y_3^2)$$

$$T_{63} = -(x_2 - x_3)(2x_2^6y_3^4 - 8x_2^5x_3y_2y_3^3 + 2x_2^5x_3y_3^4 + 3x_2^4x_3^2y_2^3y_3 + 7x_2^4x_3^2y_2y_3^3 - 4x_2^4x_3^2y_3^4 + 6x_2^4y_2^2y_3^4 - 2x_2^4y_3^6 - 2x_2^3x_3^3y_2^3y_3 - 2x_2^3x_3^3y_2y_3^3 - 16x_2^3x_3y_2^3y_3^3 - 4x_2^2x_3^4y_2^4 + 7x_2^2x_3^4y_2^3y_3 + 3x_2^2x_3^4y_2y_3^4 + 3x_2^2x_3^3y_2^5y_3 + 18x_2^2x_3^3y_2^3y_3^3 + 3x_2^2x_3^3y_2y_3^5 + 2x_2x_3^5y_2^4 - 8x_2x_3^5y_2^3y_3 - 16x_2x_3^3y_2^3y_3^3 + 2x_3^4y_2^6 + 6x_3^4y_2^4y_3^2)$$

$$T_{64} = 3x_3^2(x_2^5y_3^2 - 2x_2^4x_3y_3^3 - 2x_2^3x_3^2y_2y_3^2 + 5x_2^3x_3^2y_3^3 + 3x_2^3y_2^2y_3^3 + 3x_2^3y_3^5 + 3x_2^2x_3^3y_2^3 - 6x_2^2x_3^3y_2^2y_3 - 2x_2^2x_3^3y_3^3 - 12x_2^2x_3y_2^2y_3^3 - 2x_2^2x_3y_3^5 + 4x_2x_3^4y_2^2y_3 + 8x_2x_3^2y_2^2y_3^3 - x_3^5y_2^3 + x_3^3y_2^5 - 3x_3^3y_2^3y_3^2)$$

$$T_{65} = -x_2x_3^2(x_2 - x_3)(x_2^4y_3^3 - 2x_2^3x_3y_3^3 + 3x_2^2x_3^2y_3^3 + 3x_2^2y_2^2y_3^3 + 3x_2^2y_3^5 + 2x_2x_3^3y_2^3 - 6x_2x_3^3y_2^2y_3 - 12x_2x_3y_2^2y_3^3 + 2x_3^4y_2^3 + 6x_3^2y_2^3y_3^2)$$

$$T_{66} = -x_3(3x_2^4x_3^2y_2y_3^3 - 4x_2^4x_3^2y_3^4 - 2x_2^4y_3^6 - 6x_2^3x_3^3y_2^2y_3^2 + 10x_2^3x_3^3y_2y_3^3 + 2x_2^3x_3y_2^3y_3^3 + 6x_2^3x_3y_2y_3^5 + 3x_2^2x_3^4y_2^4 - 6x_2^2x_3^4y_2^3y_3 - 3x_2^2x_3^4y_2y_3^3 - 3x_2^2x_3^5y_3^4 - 9x_2^2x_3^2y_2^2y_3^3 - 3x_2^2x_3^2y_2y_3^5 + 4x_2x_3^5y_2^3y_3 + 8x_2x_3^3y_2^3y_3^3 - x_3^6y_2^4 + x_3^4y_2^6 - 3x_3^4y_2^4y_3^2)$$

$$T_{67} = 3x_2^2(x_2^5y_3^2 - 2x_2^4x_3y_3^3 - 4x_2^4x_2y_2y_3^2 + 2x_2^3x_3^2y_2^3 + 6x_2^3x_3^2y_2y_3^2 - 3x_2^3x_3^2y_3^3 + 3x_2^3y_2^2y_3^3 - x_2^3y_3^5 - 5x_2^2x_3^3y_2^3$$

IJESRT is licensed under a Creative Commons Attribution 4.0 International License.

ISSN: 2277-9655
Impact Factor: 5.164
CODEN: IJESS7

$$+2x_2^2x_3^3y_2^2y_3 - 8x_2^2x_3y_2^3y_3^2 - 2x_2^3x_3y_2^2y_3^3 + 2x_2x_3^4y_2^3 + 2x_2x_3^2y_2^5 + 12x_2x_3^2y_2^3y_3^2 - x_3^5y_2^3 - 3x_3^3y_2^5 - 3x_3^3y_2^3y_3^2)$$

$$T_{68} = -x_2^2x_3(x_2 - x_3)(2x_2^4y_3^3 - 6x_2^3x_3y_2y_3^2 + 2x_2^3x_3y_3^3 + 3x_2^2x_3^2y_2^3 + 6x_2^2y_2^2y_3^3 - 2x_2x_3^3y_2^3 - 12x_2x_3y_2^3y_3^2 + 3x_3^2y_2^5 + x_3^4y_2^3 + 3x_3^2y_2^3y_3^2)$$

$$T_{69} = -x_2(x_2^6y_3^4 - 4x_2^5x_3y_2y_3^3 + 3x_2^4x_3^2y_2^2y_3 + 6x_2^4x_2^2y_2y_3^3 - 3x_2^4x_3^2y_3^4 + 3x_2^4y_2^2y_3^4 - x_2^4y_3^6 - 10x_2^3x_3^3y_2^3y_3 + 6x_2^3x_3^3y_2^2y_3^2 - 8x_2^3x_3y_2^3y_3^3 + 4x_2^2x_3^4y_2^4 - 3x_2^2x_3^4y_2^3y_3 + 3x_2^2x_3^2y_2^5y_3 + 9x_2^2x_3^2y_2^3y_3^3 - 6x_2x_3^3y_2^5y_3 - 2x_2x_3^3y_2^3y_3^3 + 2x_3^4y_2^6)$$

$$T_{71} = 2(x_2 - x_3)(x_2y_3 - x_3y_2)(5x_2^3y_2^2y_3 - x_2^3y_2y_3^2 - x_2^3y_3^3 - 3x_2^2x_3y_2^3 - 3x_2^2x_3y_2^2y_3 - 3x_2^2x_3y_2y_3^2 + 3x_2x_3^2y_2^2y_3 + 3x_2x_3^2y_2y_3^2 + 3x_2x_3^2y_3^3 + 3x_2y_2^4y_3 - 3x_2y_2^2y_3^2 - 2x_2y_2^2y_3^3 + x_2y_2y_3^4 + x_2y_3^5 + x_3^3y_2^3 + x_3^3y_2^2y_3 - 5x_3^3y_2y_3^2 - x_3y_2^5 - x_3y_2^4y_3 + 2x_3y_2^3y_3^2 + 3x_3y_2^2y_3^3 - 3x_3y_2y_3^4)$$

$$T_{72} = -(x_2y_3 - x_3y_2)(2x_2^4y_2y_3^3 - x_2^4y_3^4 - 5x_2^3x_3y_2^3y_3 + 6x_2^3x_3y_2^2y_3^2 - 5x_2^3x_3y_2y_3^3 + 3x_2^2x_3^2y_2^4 + 3x_2^2x_3^2y_3^4 + 2x_2^2y_2^3y_3^3 - 3x_2^2y_2^2y_3^4 - x_2^2y_3^6 - 5x_2x_3^3y_2^3y_3 + 6x_2x_3^3y_2^2y_3^2 - 5x_2x_3^3y_2y_3^3 - 3x_2x_3y_2^5y_3 + 6x_2x_3y_2^4y_3^2 - 6x_2x_3y_2^3y_3^3 + 6x_2x_3y_2^2y_3^4 - 3x_2x_3y_2y_3^5 - x_3^4y_2^4 + 2x_3^4y_2^3y_3 + x_3^2y_2^6 - 3x_3^2y_2^4y_3^2 + 2x_3^2y_2^3y_3^3)$$

$$T_{73} = y_2y_3(y_2 - y_3)(x_2y_3 - x_3y_2)(5x_2^3y_2y_3 - 3x_2^3y_3^2 - 3x_2^2x_3y_2^2 - 3x_2^2x_3y_2y_3 + 3x_2x_3^2y_2y_3 + 3x_2x_3^2y_3^2 + 3x_2y_2^3y_3 - 5x_2y_2^2y_3^2 + x_2y_2y_3^3 + x_2y_3^4 + 3x_3^3y_2^2 - 5x_3^3y_2y_3 - x_3y_2^4 - x_3y_2^3y_3 + 5x_3y_2^2y_3^2 - 3x_3y_2y_3^3)$$

$$T_{74} = -2y_3^2(x_2y_3 - x_3y_2)(x_2^3y_3^2 + 3x_2^2x_3y_2y_3 - 3x_2x_3^2y_3^2 + 3x_2y_2^2y_3^2 - x_2y_3^4 - 6x_3^3y_2^2 + 5x_3^3y_2y_3 + x_3y_2^3y_3 - 6x_3y_2^2y_3^2 + 3x_3y_2y_3^3)$$

$$T_{75} = y_3(x_2y_3 - x_3y_2)(x_2^4y_3^3 + x_2^3x_3y_2y_3^2 - 3x_2^2x_3^2y_3^3 + 3x_2^2y_2^2y_3^3 - x_2^2y_3^5 - 6x_2x_3^3y_2^2y_3 + 5x_2x_3^3y_2y_3^2 - x_2x_3y_2^3y_3^2 - 6x_2x_3y_2^2y_3^3 + 3x_2x_3y_2y_3^4 + 2x_3^4y_2^3 + 2x_3^2y_2^3y_3^2)$$

$$T_{76} = -y_2y_3^2(x_2y_3 - x_3y_2)(x_2^3y_3^2 - 3x_2^2x_3y_2y_3 + 3x_2x_3^2y_3^2 - x_2y_2^2y_3^2 + x_2y_3^4 + 4x_3^3y_2^2 - 5x_3^3y_2y_3 - x_3y_2^3y_3 + 4x_3y_2^2y_3^2 - 3x_3y_2y_3^3)$$

$$T_{77} = -2y_2^2(x_2y_3 - x_3y_2)(5x_2^3y_2y_3 - 6x_2^3y_3^2 - 3x_2^2x_3y_2^2 + 3x_2x_3^2y_2y_3 + 3x_2y_2^3y_3 - 6x_2y_2^2y_3^2 + x_2y_2y_3^2 + x_3^3y_2^2 - x_3y_2^4 + 3x_3y_2^2y_3^2)$$

$$T_{78} = y_2(x_2y_3 - x_3y_2)(2x_2^4y_3^3 + 5x_2^3x_3y_2^2y_3 - 6x_2^3x_3y_2y_3^2 - 3x_2^2x_3^2y_3^3 + 2x_2^2y_2^2y_3^3 + x_2x_3^3y_2^2y_3 - 6x_2x_3y_2^3y_3^2 + 3x_2x_3y_2^4y_3 - x_2x_3y_2^2y_3^3 + x_3^4y_2^3 - x_3^2y_2^5 + 3x_3^2y_2^3y_3^2)$$

$$T_{79} = y_3y_2^2(x_2y_3 - x_3y_2)(5x_2^3y_2y_3 - 4x_2^3y_3^2 - 3x_2^2x_3y_2^2 + 3x_2x_3^2y_2y_3 + 3x_2y_2^3y_3 - 4x_2y_2^2y_3^2 + x_2y_2y_3^3 - x_3^3y_2^2 - x_3y_2^4 + x_3y_2^2y_3^2)$$

$$T_{81} = -6(x_2 - x_3)(y_2 - y_3)(x_2y_2 - x_3y_3)(x_2y_3 - x_3y_2)^2$$

$$T_{82} = (x_2 - x_3)(x_2y_3 - x_3y_2)^2(x_2^2y_3^2 - 3x_2x_3y_2^2 + x_3^2y_2^2 + 4x_2x_3y_2y_3 - 3x_2x_3y_3^2)$$

$$T_{83} = -(y_2 - y_3)(x_2y_3 - x_3y_2)^2(3x_2^2y_2y_3 - x_2^2y_3^2 - 4x_2x_3y_2y_3 - x_3^2y_2^2 + 3x_3^2y_2y_3)$$

$$T_{84} = 6x_3y_3(x_2y_3 - x_3y_2)^2(x_2y_3 - x_3y_2 - x_3y_3)$$

$$T_{85} = -x_3(x_2y_3 - x_3y_2)^2(2x_2^2y_3^2 - 3x_2x_3y_3^2 - x_3^2y_2^2 + 2x_2x_3y_2y_3)$$

$$T_{86} = y_3(x_2y_3 - x_3y_2)^2(x_2^2y_3^2 + 3x_3^2y_2y_3 - 2x_3^2y_2^2 - 2x_2x_3y_2y_3)$$

$$T_{87} = -6x_2y_2(x_2y_3 - x_3y_2)^2(x_2x_3 - x_2y_3 - x_3y_2)$$

$$T_{88} = -x_2(x_2y_3 - x_3y_2)^2(x_2^2y_3^2 + 3x_2x_3y_2^2 - 2x_3^2y_2^2 - 2x_2x_3y_2y_3)$$

$$T_{89} = -y_3(x_2y_3 - x_3y_2)^2(3x_2^2y_2y_3 - 2x_2^2y_3^2 - 2x_2x_3y_2y_3 + x_3^2y_2^2)$$

$$T_{91} = 2(x_2 - x_3)(x_2y_3 - x_3y_2)(x_2^5y_3 - 3x_2^4x_3y_2 + x_2^4x_3y_3 + 3x_2^3x_3^2y_2 - 2x_2^3x_3^2y_3 + 3x_2^3y_2^2y_3 - x_2^3y_3^3 + 2x_2^2x_3^3y_2 - 3x_2^2x_3^3y_3 - 5x_2^2x_3y_2^3 + 3x_2^2x_3y_2^2y_3 - 3x_2^2x_3y_2y_3^2 - x_3^2x_3y_3^3 - x_2x_3^4y_2 + 3x_2x_3^4y_3 + x_2x_3^2y_2^2 + 3x_2x_3^2y_2^2y_3 - 3x_2x_3^2y_2y_3^2 + 5x_2x_3^2y_3^3 - x_3^5y_2 + x_3^3y_2^3 - 3x_3^3y_2y_3^2$$

$$T_{92} = x_2x_3(x_2 - x_3)(x_2^4y_3 - 3x_2^3x_3y_2 + x_2^3x_3y_3 + 5x_2^2x_3^2y_2 - 5x_2^2x_3^2y_3 + 3x_2^2y_2^2y_3 - 3x_2^2y_3^3 - x_2x_3^3y_2 + 3x_2x_3^3y_3 - 5x_2x_3y_2^3 + 3x_2x_3y_2^2y_3 - 3x_2x_3y_2y_3^2 + 5x_2x_3y_3^3 - x_3^4y_2 + 3x_3^2y_2^3 - 3x_3^2y_2y_3^2$$

$$T_{93} = (x_2y_3 - x_3y_2)(x_2^6y_3^2 - 3x_2^5x_3y_2y_3 + 6x_2^4x_3^2y_2y_3 - 3x_2^4x_3^2y_3^2 + 3x_2^4y_2^2y_3^2 - x_2^4y_3^4 + 2x_2^3x_3^3y_2^2 - 6x_2^3x_3^3y_2y_3 + 2x_2^3x_3^3y_3^2 - 5x_2^3x_3y_2^3y_3 - 5x_2^3x_3y_2y_3^3 + 2x_2^3x_3y_3^4 - 3x_2^2x_3^4y_2^2 + 6x_2^2x_3^4y_2y_3 + 6x_2^2x_3^2y_2^3y_3 + 6x_2^2x_3^2y_2y_3^3 - 3x_2x_3^5y_2y_3 + 2x_2x_3^3y_2^4 - 5x_2x_3^3y_2^3y_3 - 5x_2x_3^3y_2y_3^2 + x_2^6y_2^2 - x_2^4y_2^4 + 3x_3^4y_2^2y_3^2)$$

$$T_{94} = 2x_3^2(x_2y_3 - x_3y_2)(x_2^3x_3y_3 + 3x_2^2x_3^2y_2 - 6x_2^2x_3^2y_3 - 6x_2^2y_3^3 + 3x_2x_3^3y_3 + 3x_2x_3y_2^2y_3 + 5x_2x_3y_3^3 - x_3^4y_2 + x_3^2y_2^3 - 3x_3^2y_2y_3^2)$$

IJESRT is licensed under a Creative Commons Attribution 4.0 International License.

ISSN: 2277-9655
Impact Factor: 5.164
CODEN: IJESS7

$$T_{95} = -x_2x_3^2(x_2y_3 - x_3y_2)(x_2^3x_3y_3 + x_2^2x_3^2y_2 - 4x_2^2x_3^2y_3 - 4x_2^2y_3^3 + 3x_2x_3^3y_3 + 3x_2x_3y_2^2y_3 + 5x_2x_3y_3^3 - x_3^4y_2 - x_3^2y_2^3 - 3x_3^2y_2y_3^2)$$

$$T_{96} = x_3(x_2y_3 - x_3y_2)(x_2^3x_3^2y_2y_3 - 2x_2^3x_3^2y_3^2 - 2x_2^3y_3^4 - 3x_2^2x3_3\ y2_2 + 6x_2^2x_3^3y_2y_3 + 6x_2^2x_3y_2y_3^3 - 3x_2x_3^4y_2y_3 - x_2x_3^2y_2^3y_3 - 5x_2x_3^2y_2y_3^3 + x_3^5y_2^2 - x_3^3y_2^4 + 3x_3^3y_2^2y_3^2)$$

$$T_{97} = -2x_2^2(x_2y_3 - x_3y_3)(x_2^4y_3 - 3x_2^3x_3y_2 + 6x_2^2x_3^2y_2 - 3x_2^2x_3^2y_3 + 3x_2^2y_2^2y_3 - x_2^2y_3^3 - x_2x_3^3y_2 - 5x_2x_3y_2^3 - 3x_2x_3y_2y_3^2 + 6x_2^2y_2^3)$$

$$T_{98} = x_2^2x_3(x_2y_3 - x_3y_2)(x_2^4y_3 - 3x_2^3x_3y_2 + 4x_2^2x_3^2y_2 - x_2^2x_3^2y_3 + 3x_2^2y_2^2y_3 + x_2^2y_3^3 - x_2x_3^3y_2 - 5x_2x_3y_2^3 - 3x_2x_3y_2y_3^2 + 4x_3^2y_2^3)$$

$$T_{99} = x_2(x_2y_3 - x_3y_2)(x_2^5y_3^2 - 3x_2^4x_3y_2y_3 + 6x_2^3x_3^2y_2y_3 - 3x_2^3x_3^2y_3^2 + 3x_2^3y_2^2y_3^2 - x_2^3y_3^4 - 2x_2^2x_3^3y_2^2 + x_2^2x_3^3y_2y_3 - 5x_2^2x_3y_2^3y_3 - x_2^2x_3y_2y_3^3 + 6x_2x_3^2y_2^3y_3 - 2x_3^3y_2^4)$$

REFERENCES

[1] DE BACKER, S.M., (1947). Rain and Thunderstorms in Chad – SAO/NASA Astrophysics Data System (ADS) - Heaven and Earth, Vol. 63, P.23.
[2] ODUL P., (1996). (2001). Mortar Tile Roofing – Production and Implementation. BIT (Geneva). 60 p.
[3] JEN-LOUIS FANCHON, Mechanical Guide, Nathan, ISBN 2-0-178965-8), p. 265-396.
[4] J. CHASKALOVIC, Finite Element Method for Engineering Sciences (2004), Ed. Lavoisier. (ISBN 2-7430-0708-7).
[5] K. J. BATHE, Numerical methods in finite element analysis, Prentice-Hall (1976) (ISBN 0136271901).
[6] J. C. CUILLIERE, Introduction to the Finite Element Method - 2nd Edition (2016), Ed. Dunod. (ISBN 2100742620).
[7] O. C. ZIENKIEWICZ, R. L. TAYLOR, J. Z. ZHU, The Finite Element Method: Its Basis and Fundamentals, Butterworth-Heinemann ; 6e edition (21 mars 2005) (ISBN 0750663200).
[8] PETER FRITZON ; Principles of Objet Oriented Modeling and Simulation with Modelica, Hoboken, John Wiley & Sons, Wiley (2014).
[9] GUILLAUME DUBOIS, Digital Simulation: Challenges and Good Practices for Industry, Dunod (2016).
[10] G. ALLAIRE AND A. CRAIG, Numerical Analysis and Optimization: An Introduction to Mathematical Modeling and Numerical Simulation.
[11] JOHN WALKER, Autodesk Robot Structural Analysis Professional, 2016 version, Autodesk (NASDAQ: ADSK) Creative Software and Digital Content Publishing Company, https://wikipedia.org/wiki/Autodesk,San Raphael, California, USA.
[12] [CHU-KIA WANG: Matrix methods of structural analysis, International Textbook Co; 2e edition (1970) (ISBN 0700222677).
[13] N. WILLEMS: Matrix analysis for structural engineers, Prentice-Hall (1968) (ISBN 0135654998).
[14] YAMBA & al. (1997). Vibrating Mortar Tiles – Normative Document. Project LOCOMAT. Ministry of the infrastructures of the housing environnement and the town planning- Burkina Faso.
[15] RENONET KARKA BOZABE, Chakirou Akanho TOUKOUROU, Gerard A. GBAGUIDI and Mahouton Norbert HOUNKONNOU. «Tests of quality control of the mechanical characteristics for the tiles, large format in micro-concrete: Study and realization». Africa Science, Vol.8, N°3 (2012), 1 September 2012, http://www.afriquescience.info/document.php?id=2542. ISSN 1813-548X.
[16] BOZABE R. KARKA, AHOUANNOU CLEMENT et al. , Comparative study by digital mechanical simulation of the behavior of tiles in micro-concrete, small and wide size, International Journal f Development Research, vol. 3, Issue, 06, pp. 005-016, June, 2013.
D. SPENLE, R. GOURHANT, (2003). Mechanical Calculation Guide, Hachette, (ISBN 2-01-16-8835-3), p. 130-208.
[17] MICHEL CAZENAVE, (2010,2013). Finite Element Method, Practical Approach to Structural Mechanics, 2nd edition Dunod, Paris, ISBN 978-2-10-058536-6.
[18] GAY D. And GAMBELIN J., (1999). Sizing of structures – HERMES Sciences Publications, Paris.
[19] JEAN-CHARLES CRAVEUR, (2008). Finite Element Modeling, Courses and Exercises, 3rd edition Dunod, Paris, 2011, ISBN 978-2-10-052126-5.

IJESRT is licensed under a Creative Commons Attribution 4.0 International License.